PHYSICAL REVIEW B **79**, 121403(R) (2009)

Superstructure in the termination of CoO(111) surfaces: Low-energy electron diffraction and scanning tunneling microscopy

W. Meyer, K. Biedermann, M. Gubo, L. Hammer, and K. Heinz
Lehrstuhl für Festkörperphysik, Universität Erlangen-Nürnberg, Staudtstr. 7, D-91058 Erlangen, Germany
(Received 10 February 2009; published 31 March 2009)

The surface structures of CoO(111) films epitaxially grown on Ir(100)$-(1\times1)$ are investigated by means of quantitative low-energy electron diffraction and scanning tunneling microscopy. A $(\sqrt{3}\times\sqrt{3})R30°$ superstructure is revealed for the films' ground states. It appears for film thicknesses $\geq$10 Å both for strained and unstrained films and so most likely applies also to the (111) surface of a bulk CoO crystal. The superstructure is interpreted as a stress-relieving reaction to the switch from rocksalt-type to wurtzite-type stacking below the surface which has been detected earlier.

DOI: 10.1103/PhysRevB.79.121403 PACS number(s): 68.47.Gh, 68.65.−k, 68.55.at, 61.05.jh

As is well known, transition-metal oxides play an important role in catalysis and modern material science. Concerning the latter the importance holds in particular for magnetoelectronic applications as, for example, spin valves and giant magnetoresistance devices as well as for beating the superparamagnetic limit of small clusters of a ferromagnetic material. Thereby, the phenomenon of exchange bias[1,2] is exploited, i.e., the shift of the magnetic hysteresis loop along the field axis and enhancement of the coercive field. This is observed in coupled ferromagnetic and antiferromagnetic thin films and is an interfacial phenomenon, i.e., interface properties have an essential influence on the device properties. These properties include the crystallographic structure of the interface as well as the interface roughness, that is, deviations from an atomically smooth interface.[3] It is common knowledge that the structure and roughness of catalyst surfaces are also essential for their catalytic activity.

In this Rapid Communication we address the surface of CoO(111) films. CoO plays an important role in the application and research of magnetoelectronic devices[3–8] and catalysts (e.g., Ref. 9). Recently we have shown that films grown on an unreconstructed Ir(100) surface are terminated by a wurtzite-type stacking of layers in contrast to the rocksalt-type stacking in native CoO(111) and leading to a metallic surface.[10] Here we show that this termination in its low-temperature ground state (below 50 °C) exhibits a $(\sqrt{3}\times\sqrt{3})R30°$ superstructure with respect to the (111) bulk layer unit cell of CoO. We regard this structure to be of importance as it should influence both catalytic and interfacial properties. Both the wurtzite-type termination and the $(\sqrt{3}\times\sqrt{3})R30°$ superstructure prevail in the thickness regime investigated, i.e., from 10 Å to values as large as 150 Å. Consequently, this special surface structure must be regarded as typical for CoO(111) thin films and most likely also for the (111) surface of a CoO crystal. It possibly represents a new kind of stoichiometry-saving polarity compensation so far not known from the literature (for a review, see Ref. 11).

Quantitative low-energy electron diffraction (LEED) and scanning tunneling microscopy (STM) were used to investigate the films within a two-stage ultrahigh vacuum apparatus as described earlier.[10] STM images were taken for the sample at room temperature. LEED intensity vs energy spectra, $I(E)$, were measured for normal incidence of the electron beam. The sample was cooled to liquid nitrogen temperature in order to reduce thermal diffuse scattering. A computer-controlled video method was used to record the different beam spectra.[12] They were quantitatively analyzed by application of the perturbation method TensorLEED (Refs. 12–14) using the code TENSERLEED.[15] For the structural search a frustrated annealing procedure[16] was applied controlled by the Pendry R factor which compares spectra quantitatively.[17] A maximum of 14 phase shifts calculated after Ref. 18 and corrected for thermal diffuse scattering was used. Electron attenuation was simulated as usual by an optical potential, V_{0i}=4.0 eV. The real part of the inner potential was taken to be energy dependent according to Ref. 18 in order to account for the energy dependence of the exchange-correlation potential. As the STM images reveal well-ordered surfaces, no defects—as, e.g., vacancies— were needed to be considered in the analysis.

The films investigated were grown on the unreconstructed (100) surface of iridium, Ir(100)$-(1\times1)$, which can be prepared as a metastable phase[19–21] and is stabilized by adsorbates. The preparation was performed by reactive deposition of cobalt under oxygen-rich conditions as described earlier.[10,22,23] At first, spinel-type Co_3O_4(111) films develop[24] which lose oxygen upon annealing and so transform to CoO(111) films. These exhibit a (1×1) structure at elevated temperatures but reversibly transform to a $(\sqrt{3}\times\sqrt{3})R30°$ superstructure with the temperature falling below 50 °C so that this must be considered as the films' ground state. For thicknesses below about 17 Å the unit cell is slightly distorted off ideal hexagonality due to the films' accommodation to the quadratic substrate. With increasing thickness this distortion disappears and the film relaxes by the development of misfit dislocations until eventually a flat, incommensurate, and ideally hexagonal film is established.[23] The corresponding LEED pattern is displayed in Fig. 1 with the unit cell of CoO(111) (full lines) and that of its $(\sqrt{3}\times\sqrt{3})R30°$ superstructure (broken lines) inserted for two orthogonal domains which form due to the substrate's fourfold symmetry. The whole scenario of phases developing for different film thicknesses and annealing temperatures is described in detail in Ref. 23, yet here the essentials given so far are sufficient.

The $(\sqrt{3}\times\sqrt{3})R30°$ phase was investigated for films of different thicknesses. A typical STM image as displayed in

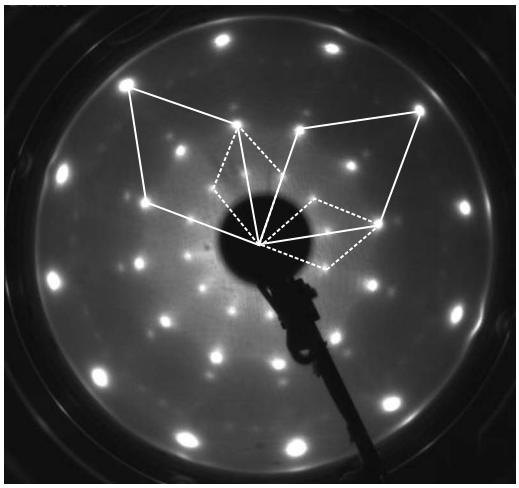

FIG. 1. LEED pattern at 125 eV of a CoO(111) film of about 130 Å thickness. The hexagonal unit cells of CoO(111) and of its $(\sqrt{3}\times\sqrt{3})R30°$ superstructure are inserted for the two orthogonal domains (full and broken lines, respectively).

Fig. 2 shows a lattice plane which is not atomically flat but exhibits some buckling. The superstructure unit cell contains three atoms within this layer. One of them appears to protrude from the surface by 0.1 Å as estimated from the corresponding vertical displacement of the STM tip (neglecting electronic effects). The precise and full structure, in particular concerning layers deeper in the surface, comes by the LEED structure determination. We concentrate on a film of about 130 Å thickness which is practically ideally hexagonal. Its lateral lattice parameter is already very close to that of bulk CoO, i.e., a_p=3.028 Å as determined for the (1×1) phase of a film of the same thickness.[10,23] Intensity data of seven integers and five fractional order spots entered the analysis with database widths on the energy scale of ΔE_i=2400 eV and ΔE_f=1300 eV, respectively, so that the total database is as large as $\Delta E=\Delta E_i+\Delta E_f$=3700 eV. The starting point of the structural search was the structure retrieved for the (1×1) phase which prevails above 50 °C and which is terminated by wurtzitelike stacking of layers[10] with oxygen in the top layer. It is illustrated in panels (a) and (b) of Fig. 3 in perspective and on-top view, respectively. For the LEED analysis of the $(\sqrt{3}\times\sqrt{3})R30°$ superstructure only

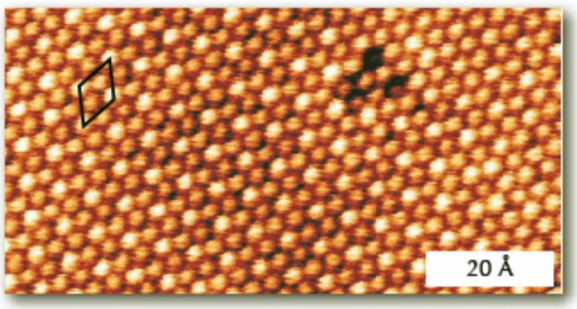

FIG. 2. (Color online) STM image of the $(\sqrt{3}\times\sqrt{3})R30°$ superstructure (film thickness of ≈15 Å; U=−0.102 V and I=9.51 nA).

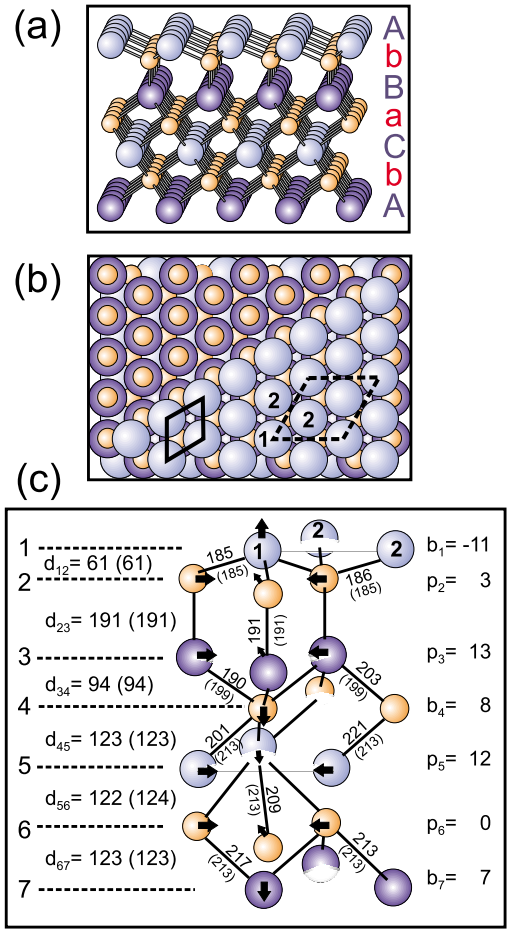

FIG. 3. (Color online) Structural models of CoO(111) films: panels (a) and (b) display the stacking sequence with a wurtzite-type slab terminating the surface in perspective and top view with oxygen (cobalt) represented by large (small) spheres. Panel (c) visualizes the $(\sqrt{3}\times\sqrt{3})R30°$ superstructure developing from the atomic positions in (a) and (b) by atomic movements as indicated by arrows [the (1×1) and $(\sqrt{3}\times\sqrt{3})R30°$ cells are given in (b) by full and broken lines, respectively]. The buckling amplitudes b_i and in-plane trimerization shifts p_i are counted as positive due to shifts into the surface and onto each other. The interlayer spacings $d_{i,i+1}$ are with respect to the center of mass planes. The resulting Co-O bond lengths are also inserted. Values in brackets are for the (1×1) phase. All numbers are in pm units.

atomic displacements saving the threefold rotational symmetry were allowed as indicated by arrows in panel (c). This allows for buckling amplitudes b_i or in-plane trimerization displacements p_j in different layers [the reader should note that due to symmetry arguments only two of the atoms in the supercell are different as indicated by labels 1 and 2 in the top layer of panels (b) and (c) of the figure]. Of course, the spacings between layers, $d_{i,i+1}$ (here given with respect to their center of mass planes) can be modified, too.

An excellent fit between measured and computed intensities results for the scenario displayed in Fig. 3(c). It turns out that the top (oxygen) layer is buckled, the two following layers undergo in-plane trimerization displacements, etc. The Co-O bond lengths calculated from the parameters determined are also inserted. In all cases (when applying) the

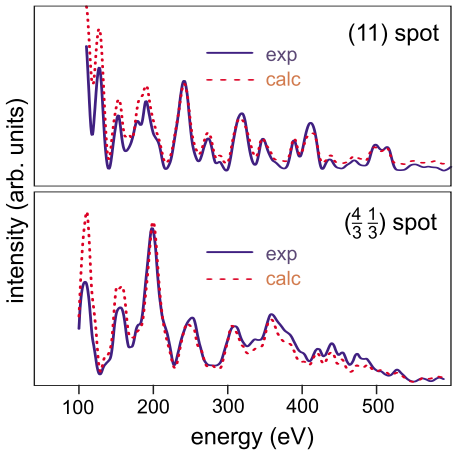

FIG. 4. (Color online) Comparison of experimental and best-fit calculated LEED spectra for two selected beams.

values determined for the (1×1) phase (above 50 °C and as taken from Ref. 10) are added in brackets for comparison. The best-fit Pendry R factor is $R=0.110$ with $R_i=0.101$ ($R_f=0.138$) for the subset of integer (fractional) order spots. This is remarkably low for a superstructure of the complexity described. The low R factor is consistent with an equally favorable optical comparison of computed and measured data as demonstrated in Fig. 4 for two selected beams. The variance in the R factor, $\mathrm{var}(R)=R\sqrt{8V_{0i}/\Delta E}=0.010$, is also very low, equivalent to low error limits for the model parameters determined. Neglecting parameter correlations they are estimated to be ±0.02 Å for buckling amplitudes and interlayer spacings and ±0.05 Å for in-plane trimerization shifts. It is also worth noting that the experimental ratio between average intensities of fractional and integer order spots (0.117) is very close to the calculated value (0.127) in agreement with the almost perfect structural order in the STM images.

As displayed in Fig. 3(c) the interlayer spacings of the reconstructed and unreconstructed surfaces are identical well within the limits of errors. Also, the rocksalt-type Co-O bond lengths below the fifth layer change only little, i.e., by less than 2%, and are close to the value in bulk CoO (2.13 Å). Small bond-length modifications (again by less than 2%) hold also within the top three layers (which are of wurtzite type) in spite of the 0.11 Å buckling in the top layer which is in agreement with the STM result. Unfortunately, there is no safe literature value for the bond length in bulk wurtzite CoO for comparison. An early investigation of small crystals finds a value of 1.97 Å,[25] and more recent experimental work (again for small crystals) reports a distorted structure with an axial bond length of 2.165 Å and a more "equatorial" Co-O distance of 1.923 Å.[26] In contrast, recent calculations applying density-functional theory (DFT) (Ref. 27) find that wurtzite-type CoO structures should relax to a configuration with Co and O lying in the same plane with an axial bond length of 2.146 Å and an equatorial value of 2.007 Å. Our values (1.91 Å for the axial length and 1.85–1.86 Å for the equatorial one) are rather different from the values reported, not surprisingly in view of the match to the rocksalt phase and possible surface relaxations involved. Due to the lattice parameter of the rocksalt planes ($a_R\approx3.03$ Å) and the corresponding value reported for wurtzite CoO [which varies between 3.21 (Ref. 25) and 3.476 Å (Ref. 27)] the wurtzite slab is under compressive stress corresponding to a strain in the range of 5.6%–12.8%.

The only considerable bond-length changes [up to more than 5% with respect to the (1×1) phase] are observed between the third and fifth layers wherein region can be considered as the interface between the rocksalt and wurtzite CoO. Possibly these changes are stress induced with the reconstructive atomic movements reducing the stress. The in- and out-of-plane movements proceed to the surface where the atoms are free to assume the chemically optimal bond length. However this is at the price of an enlarged, i.e., $(\sqrt{3}\times\sqrt{3})R30°$ unit cell with the top layer buckled by 0.11 Å. As this buckling eventually is interface driven it should—in contrast to surface reconstructions driven by surface bond truncation—largely prevail when the surface gets in contact with other layers, e.g., when CoO(111) is used in magnetoelectronic devices. Then the microroughness of the surface should modify the magnetic properties. The latter might also be influenced by the different volumes of the cobalt ions at the rocksalt/wurtzite interface (as taken from the different bond lengths involved) indicating that they may accommodate different spins. Of course, in the absence of reliable first-principles calculations all these interpretations are rather speculative.

The $(\sqrt{3}\times\sqrt{3})R30°$ superstructure was analyzed also for smaller film thicknesses including films with distorted hexagonal mesh. Their structure parameters are consistent with the symmetry break and deviate only little from those of the hexagonal structure in agreement with the only small distortion. The reconstruction obviously is an intrinsic feature of the CoO(111) films. It corresponds to their ground state as the extra spots only disappear for temperatures above 50 °C. The thickest film analyzed consists—with a thickness of 130 Å—of as much as about 50 Co-O bilayers. With its practically ideal hexagonal unit mesh it is incommensurate with the substrate and structurally not affected by it (except for the growth of two orthogonal domains of the oxide). So, the reconstruction and the wurtzite-type surface termination most likely are typical also for the (111) surface of a bulk CoO crystal. Unfortunately, investigations of such crystals are rare. Work applying x-ray diffraction reports on a CoO(111) surface terminated by a 50-Å-thick slab of Co_3O_4.[28] In contrast, a more hidden report in fact demonstrates the appearance of a $(\sqrt{3}\times\sqrt{3})R30°$ phase of CoO(111).[29] Such superstructures were reported also for other transition-metal oxides. For MnO(111) (Ref. 30) the crystallography is still unknown and so our structure might be a model candidate. For MgO(111) both stoichiometric[31] and nonstoichiometric[32] reconstructions are reported which, however, do not agree with our structural model.

The triplication of the unit cell by local displacements of ions does not change the charge accommodated in the surface, and so it cannot be responsible for polarity compensation.[11] Yet it should lower the free energy by a certain amount which, however, remains uncertain in the absence of reliable first-principles calculations.

In conclusion we claim that the crystallographic ground state of (111) surfaces of CoO thin films and most likely also of crystals are terminated by a thin slab of wurtzite-type CoO and a $(\sqrt{3}\times\sqrt{3})R30°$ surface reconstruction. The latter is characterized by a top layer buckling of 0.11 Å so that the surface is not flat on the atomic scale. This should have implications for the properties of magnetoelectronic devices in which CoO(111) is used as the antiferromagnetic thin film. Also, the rather complex structure is a test case for first-principles calculations which are nontrivial due to the highly correlated electron interactions in oxides such as CoO.[33]

The authors are indebted to Deutsche Forschungsgemeinschaft (DFG) for financial support.

[1] W. H. Meiklejohn and C. P. Bean, Phys. Rev. **102**, 1413 (1956).
[2] W. H. Meiklejohn and C. P. Bean, Phys. Rev. **105**, 904 (1957).
[3] J. Nogués and I. K. Schuller, J. Magn. Magn. Mater. **192**, 203 (1999).
[4] F. T. Parker, K. Takano, and A. E. Berkowitz, Phys. Rev. B **61**, R866 (2000).
[5] F. Radu, M. Etzkorn, R. Siebrecht, T. Schmitte, K. Westerholt, and H. Zabel, Phys. Rev. B **67**, 134409 (2003).
[6] M. Gruyters, Europhys. Lett. **64**, 803 (2003).
[7] T. Blachowicz, A. Tillmanns, M. Fraune, R. Ghadimi, B. Beschoten, and G. Güntherodt, Phys. Rev. B **75**, 054425 (2007).
[8] S. Brems, D. Buntinx, K. Temst, C. Van Haesendonck, F. Radu, and H. Zabel, Phys. Rev. Lett. **95**, 157202 (2005).
[9] *Metal Oxide Catalysis*, edited by S. D. Jackson and J. S. J. Hargreaves (Wiley, Weinheim, Germany, 2008).
[10] W. Meyer, D. Hock, K. Biedermann, M. Gubo, S. Müller, L. Hammer, and K. Heinz, Phys. Rev. Lett. **101**, 016103 (2008).
[11] J. Goniakowski, F. Finocchi, and C. Noguera, Rep. Prog. Phys. **71**, 016501 (2008).
[12] K. Heinz, Rep. Prog. Phys. **58**, 637 (1995).
[13] P. J. Rous, J. B. Pendry, D. K. Saldin, K. Heinz, K. Müller, and N. Bickel, Phys. Rev. Lett. **57**, 2951 (1986).
[14] P. J. Rous and J. B. Pendry, Prog. Surf. Sci. **39**, 3 (1992).
[15] V. Blum and K. Heinz, Comput. Phys. Commun. **134**, 392 (2001).
[16] M. Kottcke and K. Heinz, Surf. Sci. **376**, 352 (1997).
[17] J. B. Pendry, J. Phys. C **13**, 937 (1980).
[18] J. Rundgren, Phys. Rev. B **68**, 125405 (2003).
[19] J. Küppers and H. Michel, Appl. Surf. Sci. **3**, 179 (1979).
[20] K. Heinz, G. Schmidt, L. Hammer, and K. Müller, Phys. Rev. B **32**, 6214 (1985).
[21] D. Lerch, A. Klein, A. Schmidt, S. Müller, L. Hammer, K. Heinz, and M. Weinert, Phys. Rev. B **73**, 075430 (2006).
[22] C. Giovanardi, L. Hammer, and K. Heinz, Phys. Rev. B **74**, 125429 (2006).
[23] K. Biedermann, M. Gubo, L. Hammer, and K. Heinz, J. Phys.: Condens. Matter **21**, 185003 (2009).
[24] W. Meyer, K. Biedermann, M. Gubo, L. Hammer, and K. Heinz, J. Phys.: Condens. Matter **20**, 265011 (2008).
[25] M. J. Redman and E. G. Steward, Nature (London) **193**, 867 (1962).
[26] A. S. Risbud, L. P. Snedeker, M. M. Elcombe, A. K. Cheetham, and R. Seshadari, Chem. Mater. **17**, 834 (2005).
[27] T. Archer, R. Hanafin, and S. Sanvito, Phys. Rev. B **78**, 014431 (2008).
[28] C. Mocuta, A. Barbier, and G. Renaud, Appl. Surf. Sci. **162-163**, 56 (2000).
[29] K. Arai, S. Takatoh, T. Enokijima, T. Hayashi, T. Yikegaki, J. Tsukajima, Y. Fujimori, and S. Usami, Kanagawa Institute of Technology: Part B Technical Research, 1997, Vol. 21, p. 131 (http://www.kait-r.com:8080/dspace/bitstream/10368/783/1/kkb-021-020.pdf)
[30] F. Allegretti, C. Franchini, V. Bayer, M. Leitner, G. Parteder, B. Xu, A. Fleming, M. G. Ramsey, R. Podloucky, S. Surnev, and F. P. Netzer, Phys. Rev. B **75**, 224120 (2007).
[31] R. Plass, K. Egan, C. Collazo-Davila, D. Grozea, E. Landree, L. D. Marks, and M. Gajdardziska-Josifovska, Phys. Rev. Lett. **81**, 4891 (1998).
[32] A. Subramanian, L. D. Marks, O. Warschkow, and D. E. Ellis, Phys. Rev. Lett. **92**, 026101 (2004).
[33] U. D. Wdowik and K. Parlinski, Phys. Rev. B **75**, 104306 (2007).